DOI: 10.1002/ejic.200500526

A Terephthalato-Bridged Ni^{II} Complex Capped with a Nonchelating Ligand Displays a Three-Dimensional Supramolecular Network Constructed by Coordination and Multi-Intermolecular Forces

Chang Seop Hong,*[a] Jung Hee Yoon,[a] Jeong Hak Lim,[a] and Hyun Hee Ko[a]

Keywords: Magnetic properties / Nickel / Noncovalent interactions / O ligands / Supramolecular chemistry

A new tp-bridged complex $[Ni(pyrazole)_4(tp)]_n$ (**1**; tp = terephthalate) coordinated with a nonchelating pyrazole ligand has been synthesized and characterized using X-ray structure determination and magnetic studies. The crystal structure reveals that the capping ligand functions as a source of hydrogen bonding and intermolecular contacts, such as π–π and CH–π interactions, that result in a three-dimensional supramolecular assembly. Weak antiferromagnetic couplings are transmitted between Ni^{II} centers through the tp linkage.

Introduction

Coordination polymers have been one of the active research areas applicable to molecular magnets and functional metal–organic frameworks for storage, exchange, and separations.[1,2] The tp ligand is frequently employed in the construction of such complexes due to its diverse binding modes as a linker which allow it to form a variety of structures from discrete molecules to one- (1D), two- (2D), or three-dimensional (3D) networks.[3–7] Interestingly, the molecular dimensionality of coordination polymers bridged by tp can be raised by hydrogen bonding and other intermolecular contacts, such as face-to-face π–π and edge-to-face CH–π interactions.[8,9] The former are realized when lattice water molecules that act as hydrogen donors and acceptors are present in the crystal structures.[10] The use of aromatic bidentate moieties such as 2,2′-bypridine and 1,10-phenanthroline, which fill up coordination spaces around the metal ions, as capping ligands promotes the supramolecular contacts between the aromatic pyridyl groups, which in turn leads to increased dimensionality.[8] It is highly desirable to fabricate dehydrated supramolecular self-assemblies with all these intermolecular interactions (hydrogen bonding, π–π, and CH–π interactions) at the same time as lattice water molecules, which are sources of hydrogen bonds, are easily removed and the crystal lattice could consequently collapse. In this respect, we have selected pyrazole as a capping ligand as it possesses an N–H group for hydrogen bonding and a planar aromatic ring for the other intermolecular interactions.

Here we present the synthesis and detailed structural and magnetic characterization of a new tp-linked dehydrated Ni^{II} compound $[Ni(pyrazole)_4(tp)]_n$ (**1**), which, to the best of our knowledge, is the first example capped by a nonchelating pyrazole ligand among coordinative 1D Ni^{II} systems bridged by tp. The capping ligand plays a crucial role in the formation of the unique 3D supramolecular framework of **1** as it is connected by the combined forces of coordination as well as noncovalent hydrogen bonds and face-to-face π–π and edge-to-face CH–π interactions. Weak antiferromagnetic interactions are operative between the magnetic centers through the long tp bridge.

Results and Discussion

The reaction of Ni^{2+}, pyrazole and dipotassium terephthalate in a ratio of 1:4:1 in water led to the formation of **1**. The strong bands in the IR spectrum centered at 3370 and 3350 cm^{-1} are assigned to the characteristic N–H stretching vibrations of pyrazole, and the presence of the broad bands in the range 2900–2400 cm^{-1} are indicative of hydrogen bonds between the N–H groups of pyrazole and the carboxylate oxygens of tp. The differences (Δ) between the antisymmetric $\nu_a(CO_2^-)$ and symmetric $\nu_s(CO_2^-)$ stretching frequencies in the IR spectrum of **1** are 178 and 203 cm^{-1}. The calculated Δ values, when compared with the reference value (170 cm^{-1}) of dipotassium terephthalate, suggest that the binding mode of tp appears to be monodentate,[11] which was confirmed by X-ray analysis.

A perspective view of **1** together with the atom-labeling scheme is presented in Figure 1. Selected distances and angles are tabulated in Table 1. The specific feature is that two crystallographically different chains exist in the unit cell. Each nickel atom lies on an inversion center and exhib-

---

[a] Department of Chemistry and Center for Electro- and Photoresponsive Molecules, Korea University,
Seoul 136-701, Korea
E-mail: cshong@korea.ac.kr

its a distorted octahedral geometry consisting of four equatorial nitrogen atoms of pyrazole ligands, with an average Ni–N distance of 2.097(7) Å, and two axial oxygen atoms of the tp bridge, with an average Ni–O distance of 2.109(1) Å. For a chain including Ni1 atoms (Ni1 chain), the dihedral angle (α) between the carboxylate group and the benzene ring of the tp ligand is 21.41(28)°, whereas the other chain with Ni2 atoms (Ni2 chain) has a dihedral angle of 10.25(32)°. The benzene rings of the two chains are tilted with a dihedral angle of 77.20(13)°, and the shortest intrachain Ni···Ni distance is 11.446(2) Å for both chains.

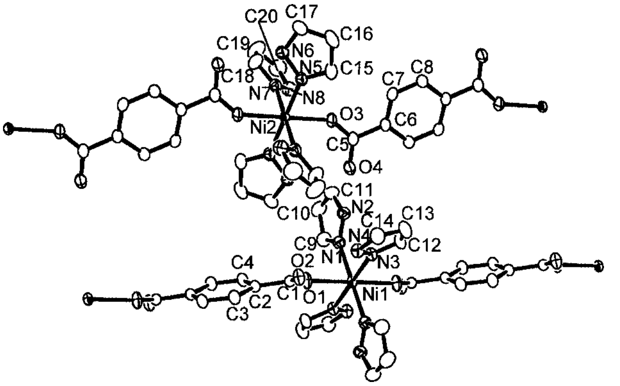

Figure 1. ORTEP diagram of **1** with the atom numbering scheme.

Table 1. Bond lengths [Å] and angles [°] for **1**.

Ni(1)–N(3)	2.0895(15)	Ni(1)–N(1)	2.1017(16)
Ni(1)–O(1)	2.1100(12)	Ni(2)–N(7)	2.0938(16)
Ni(2)–N(5)	2.1061(16)	Ni(2)–O(3)	2.1076(12)
N(3)–Ni(1)–N(1)	90.95(6)	N(3)–Ni(1)–O(1)	94.12(6)
N(1)–Ni(1)–O(1)	85.89(6)	C(1)–O(1)–Ni(1)	146.59(13)
C(9)–N(1)–Ni(1)	131.87(14)	N(2)–N(1)–Ni(1)	123.42(12)
C(12)–N(3)–Ni(1)	131.59(13)	N(4)–N(3)–Ni(1)	122.05(11)
N(7)–Ni(2)–N(5)	91.69(6)	N(7)–Ni(2)–O(3)	87.45(6)
N(5)–Ni(2)–O(3)	87.29(6)	C(5)–O(3)–Ni(2)	144.46(13)
C(15)–N(5)–Ni(2)	131.13(13)	N(6)–N(5)–Ni(2)	122.84(12)
C(18)–N(7)–Ni(2)	132.81(14)	N(8)–N(7)–Ni(2)	122.63(13)

The chains form an extended 3D network structure in which, interestingly, three types of noncovalent forces, namely hydrogen bonds, face-to-face π–π interactions, and edge-to-face CH–π interactions, are involved. As displayed in Figure 2 (a), the 3D molecular view in the *ac* plane can be described as a combination of two sheets that are slanted with respect to each other. Sheet A comprises Ni1 chains and Ni2 chains, with a shortest interchain Ni1···Ni2 distance of 8.060(1) Å (Figure 2, b). There is intrachain hydrogen bonding between unbound carboxylate oxygens and N–H groups of pyrazole in an Ni2 chain. Simultaneously, the free carboxylate oxygen atoms participate in interchain hydrogen bonds to N–H groups in other Ni1 chains, eventually generating a 3D network structure. It is worthwhile to note that interchain edge-to-face CH–π interactions become established between C14–H14 from the pyrazoles and C6-containing benzene rings (2.826 Å), as well as between C3–H3 from the benzene rings and the N5-containing pyrazole rings (3.019 Å). In sheet B, shown in Figure 2 (c), symmetry-related free carboxylate oxygen atoms in an Ni2 chain undergo intrachain and interchain hydrogen bonding to the N–H groups of the pyrazole rings in the same chain and adjacent Ni1 chains, respectively. In comparison with sheet A, sheet B consists of CH–π interactions between pyrazole rings: interchain contacts between C17–H17 from N5-containing pyrazoles and N1-containing pyrazoles (3.007 Å). The C9–H9 moiety from the N1-containing pyrazoles undergoes intrachain contacts with N3-containing pyrazole planes (2.852 Å). For sheets A and B, the distances of the hydrogen bonds are $d(\text{D}\cdots\text{A}) = 2.931(2)$ Å and $\angle(\text{D–H}\cdots\text{A}) = 134°$ for N2–H2···O4, $d(\text{D}\cdots\text{A}) = 2.711(2)$ Å and $\angle(\text{D–H}\cdots\text{A}) = 158°$ for N6–H6···O4a ($-x - 1, -y + 3, -z + 1$), $d(\text{D}\cdots\text{A}) = 2.720(2)$ Å and $\angle(\text{D–H}\cdots\text{A}) = 168°$ for

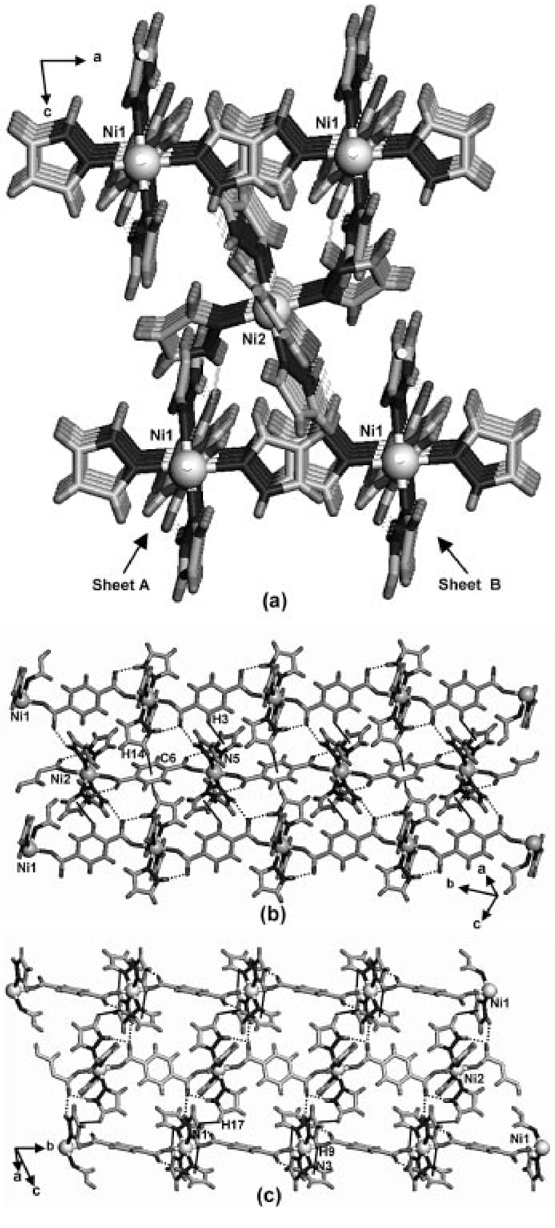

Figure 2. Extended view of **1** showing (a) a 3D network in the *ac* plane, (b) sheet A, and (c) sheet B. Progressively darker shades of grey represent Ni, C, H, N, and O, respectively. The dotted lines indicate hydrogen bonds and the solid lines denote CH–π interactions.

N4–H4A···O2, and $d(\mathrm{D}\cdots\mathrm{A})$ = 2.976(2) Å and $\angle(\mathrm{D–H}\cdots\mathrm{A})$ = 137° for N8–H8A···O2b (x – 1, y, z). As seen in Figure 3, additional noncovalent interactions correspond to face-to-face π–π stacking between aromatic pyrazole rings residing on the same type of nearest neighbor chains residing in sheets A and B, respectively, where the shortest interchain distance of Ni1(Ni2)···Ni1(Ni2) is equal to 8.467(1) Å. The pyrazole groups associated with π–π interactions are separated by 3.410–3.507 Å, which is consistent with those between 2,2′-bipyridine or 1,10-phenanthroline ligands in tp-bridged $\mathrm{Ni^{II}}$ chain compounds.[8] Thus, it should be noted that the capping pyrazole ligand plays a key role in the construction of the 3D supramolecular network structure by allowing multi-intermolecular interactions concurrently.

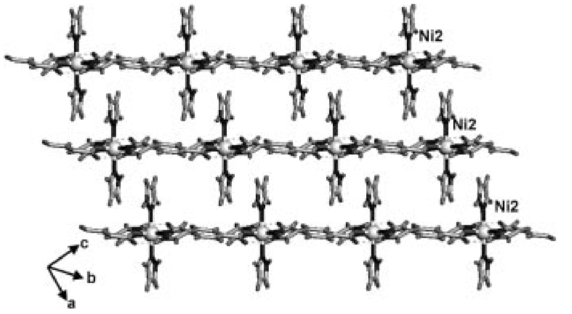

Figure 3. Extended molecular view exhibiting π–π stacking. Progressively darker shades of grey represent Ni, C, H, N, and O, respectively.

The magnetic behavior of **1** is shown in Figure 4 in the form of the temperature dependence of χ_m and $\chi_\mathrm{m}T$ at 2000 G in the temperature range 1.8–300 K. At 300 K, the $\chi_\mathrm{m}T$ value is 1.24 cm³ K mol⁻¹, which is in the usual range for a noninteracting $\mathrm{Ni^{II}}$ ion. The $\chi_\mathrm{m}T$ value decreases slowly upon cooling, then drops abruptly below 20 K, finally reaching a value of 0.45 cm³ K mol⁻¹ at 1.8 K, thus indicating the existence of an antiferromagnetic interaction between the magnetic centers. The inverse magnetic susceptibility data obey the Curie–Weiss equation [$\chi_\mathrm{m} = C/(T - \theta)$] in the linear region, giving C = 1.24 cm³ K mol⁻¹ and θ = –0.46 K. This definitely demonstrates that adjacent magnetic spins are coupled antiferromagnetically.

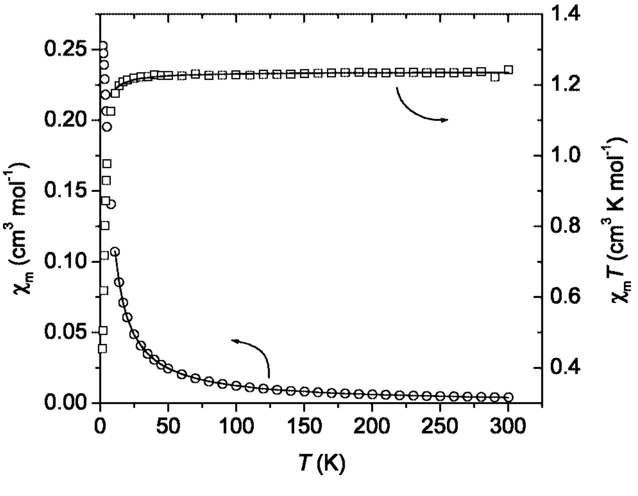

Figure 4. Plots of χ_m and $\chi_\mathrm{m}T$ vs. T for **1**. The solid lines show the best theoretical fits.

The magnetic data were fitted to the analytical expression derived by Weng on the basis of the spin Hamiltonian $H = -J\cdot\sum_i S_i\cdot S_{i+1}$, where the local anisotropy is neglected [Equation (1)].[12]

$$\chi_\mathrm{m} = \{Ng^2\beta^2/kT\}[2.0 + 0.0194x + 0.777x^2]/[3.0 + 4.346x + 3.232x^2 + 5.834x^3] \quad (1)$$

in which $x = |J|/kT$. Because this equation does not take into account the zero-field splitting or the Haldane gap, fitting was performed above 10 K. With consideration of a molecular field approximation (zJ'), the magnetic fitting given by the solid line in Figure 4 yields parameters of g = 2.224(1), J = –0.22(1) cm⁻¹, and $zJ' \approx 0$. The use of the infinite chain model derived by Fisher[13] produces similar results of g = 2.224(1), J = –0.24(1) cm⁻¹, and $zJ' \approx 0$ in the same temperature range. Thus, it is evident that a weak antiferromagnetic interaction is operative between the $\mathrm{Ni^{II}}$ centers. It is reasonable to assume that the antiferromagnetic behavior occurs via the long tp bridge because, with the given distances, intrachain interactions through covalent linkages are stronger than interchain couplings via the intermolecular contacts, which is consistent with the results reported previously for tp-linked $\mathrm{Ni^{II}}$ systems.[3,10,14,15] In comparison with the 1D $\mathrm{Ni^{II}}$ macrocyclic complex (J = –1.37 cm⁻¹), where the intrachain Ni–Ni separation is virtually the same (11.5 Å) and α is significantly smaller (5.6°), the weaker antiferromagnetic interaction ($J \approx$ –0.2 cm⁻¹) in **1** arises from the sizeable difference in α (21.41° and 10.25° for **1**).[14]

In summary, we have prepared a tp-bridged $\mathrm{Ni^{II}}$ compound with a 3D network structure built by covalent and noncovalent bonds. In particular, the nonchelating capping pyrazole ligand, which contains an N–H group and a planar aromatic ring, behaves as a unique and efficient synthon for noncovalent contacts of hydrogen bonding, face-to-face π–π interactions, and edge-to-face CH–π interactions, thus opening-up an opportunity to create a new class of supramolecular assemblies.

Experimental Section

Physical Measurements: Elemental analyses for C, H, and N were performed at the Elemental Analysis Service Center of Sogang University. Infrared spectra were obtained from KBr pellets with a Bomen MB-104 spectrometer. Magnetic susceptibilities for **1** were carried out using a Quantum Design MPMS-7 SQUID susceptometer. Diamagnetic corrections of **1** were estimated from Pascal's tables.

[Ni(pyrazole)$_4$(tp)]$_n$ (1): Pyrazole (2.0 mmol), dissolved in 5 mL of water, was added, with stirring, to a 10 mL aqueous solution of nickel(II) nitrate hexahydrate (0.50 mmol). The resultant pale-green solution was treated with a solution of potassium terephthalate (0.50 mmol) in 5 mL of water. The filtrate of the resulting solution was allowed to stand for several days to give blue crystals of **1** in 70% yield based on Ni in the presence of four equivalents of pyrazole. $C_{20}H_{20}N_8NiO_4$: calcd. C 48.5, H 4.07, N 22.6; found C 48.2, H 4.09, N 22.5. Selected IR data (KBr pellet): $\tilde{\nu}$ = 3379 cm^{-1} (m), 3350 (m), 3138 (w), 3126 (w), 3061 (w), 2595 (m, broad), 1920 (w), 1561 [s, tp $\nu_a(CO_2^-)$], 1523 (m), 1498 (w), 1452 (m), 1383, 1358 [s, tp $\nu_s(CO_2^-)$], 1279 (w), 1166 (w), 1150 (w), 1123 (m), 1059 (s), 1015 (w), 933 (m), 910 (m), 882 (m), 851 (w), 810 (s), 764 (s), 750 (s), 726 (m), 662 (w), 621 (w), 604 (m), 515 (m).

X-ray Structural Analysis: $C_{20}H_{20}N_8NiO_4$, M = 495.15, triclinic, $P\bar{1}$, a = 8.4673(14), b = 11.4460(16), c = 11.920(2) Å, α = 77.663(15)°, β = 80.088(15)°, γ = 71.529(12)°, V = 1063.6(3) Å^3, Z = 2, D_c = 1.546 g cm^{-3}, $F(000)$ = 512. Final R indices were R_1 = 0.0258, wR_2 = 0.0669 [$I > 2\sigma(I)$]. The crystal data for **1** are summarized in Table 2.

Table 2. Crystal data and structure refinement for **1**.

Empirical formula	$C_{20}H_{20}N_8NiO_4$
Formula mass	495.15
Crystal system	triclinic
Space group	$P\bar{1}$
a [Å]	8.4673(14)
b [Å]	11.4460(16)
c [Å]	11.920(2)
α [°]	77.663(15)
β [°]	80.088(15)
γ [°]	71.529(12)
V [Å^3]	1063.6(3)
Z	2
μ [mm^{-1}]	0.959
ρ [g cm^{-3}]	1.546
$F(000)$	512
Goodness-of-fit	1.051
R_1 [$I > 2\sigma(I)$]	0.0258
wR_2 [$I > 2\sigma(I)$]	0.0669

CCDC-274883 contains the supplementary crystallographic data for this paper. These data can be obtained free of charge from The Cambridge Crystallographic Data Centre via www.ccdc.cam.ac.uk/data_request/cif.

Acknowledgments

We would like to thank an Operation Program on Shared Research Equipment of KBSI and MOST. This work was financially supported by the CRM-KOSEF.

[1] O. Kahn, *Magnetism: A Supramolecular Function*, Kluwer, Dordrecht, The Netherlands, **1996**.
[2] S. Kitagawa, R. Kitaura, S.-i. Noro, *Angew. Chem. Int. Ed.* **2004**, *43*, 2334–2375.
[3] J. Cano, G. D. Munno, J. L. Sanz, R. Ruiz, J. Faus, F. Lloret, M. Julve, A. Caneschi, *J. Chem. Soc., Dalton Trans.* **1997**, 1915–1923.
[4] C. S. Hong, Y. S. You, *Polyhedron* **2004**, *23*, 3043–3050.
[5] L. Li, Z. Liu, S. S. Turner, D. Liao, Z. Jiang, S. Yan, *Eur. J. Inorg. Chem.* **2003**, 62–65.
[6] X. Shi, G. Zhu, Q. Fang, G. Wu, G. Tian, R. Wang, D. Zhang, M. Xue, S. Qiu, *Eur. J. Inorg. Chem.* **2004**, 185–191.
[7] C. S. Hong, Y. Do, *Inorg. Chem.* **1997**, *36*, 5684–5685.
[8] Y. Go, X. Wang, E. V. Anokhina, A. J. Jacobson, *Inorg. Chem.* **2004**, *43*, 5360–5367.
[9] C. Ma, Y. Han, R. Zhang, D. Wang, *Eur. J. Inorg. Chem.* **2005**, 1649–1652.
[10] C. S. Hong, Y. S. You, *Polyhedron* **2004**, *23*, 1379–1384.
[11] K. Nakamoto, *Infrared and Raman Spectra of Inorganic and Coordination Compounds: Part B: Applications*, in *Coordination, Organometallic, and Bioinorganic Chemistry*, 5th ed, John Wiley & Sons, Inc: New York, **1997**.
[12] A. Meyer, A. Gleizes, J.-J. Girerd, M. Verdaguer, O. Kahn, *Inorg. Chem.* **1982**, *21*, 1729–1739.
[13] M. E. Fisher, *Am. J. Phys.* **1964**, *32*, 343–346.
[14] K.-Y. Choi, K. M. Chun, I.-H. Suh, *Polyhedron* **2001**, *20*, 57–65.
[15] K.-Y. Choi, K. M. Chun, K.-C. Lee, J. Kim, *Polyhedron* **2002**, *21*, 1913–1920.

Received: June 13, 2005